VSP

Advanced Composite Materials 17 (2008) 319–332

ADVANCED COMPOSITE MATERIALS
www.brill.nl/acm

Thermoelastic Behaviors of Fabric Membrane Structures

Jin-Ho Roh [a,b], **Han-Geol Lee** [c] **and In Lee** [a,*]

[a] Department of Aerospace Engineering, Korea Advanced Institute of Science and Technology, 373-1 Guseong-dong, Yuseong-gu, Daejeon 305-701, Korea

[b] Present address: School of Aerospace and Mechanical Engineering, Korea Aerospace University, 200-1, Hwajeon-dong, Deogyang-gu, Goyang-city, Geonggi-do, 412-791, Korea

[c] P/T NVH Team, GM Daewoo Auto and Technology, 199-1 Cheongcheon-dong, Bupyeong-gu, Incheon 403-714, Korea

Received 27 August 2007; accepted 24 December 2007

Abstract

The thermoelastic behaviors of an inflatable fabric membrane structure for use in a stratospheric airship envelope are experimentally and numerically investigated. Mechanical tensile properties of the membrane material at room, high, and low temperatures are measured using an Instron® universal testing machine and an Instron® thermal chamber. To characterize the nonlinear behavior of the inflated membrane structure due to wrinkling, the bending behavior of an inflated cylindrical boom made of a fabric membrane is observed at various pressure levels. Moreover, the envelope of a stratospheric airship is numerically modeled based on the thermoelastic properties of the fabric membrane obtained from experimental data, and the wrinkled deformed shape induced by a thermal load is analyzed.

Keywords

Thermoelastic behaviors, inflatable structures, fabric membrane, stratospheric airship, wrinkling

1. Introduction

Recently, interest has grown in developing unmanned stratospheric airships to be utilized as telecommunication relays, for environmental monitoring, or for surveillance purposes. Due to their greatly expected usage, many countries have plans to develop such airships [1]; for example, Korean researchers flew scaled-down, 50–60 m class unmanned airships as a technical demonstration [2]. Airships are typically huge structures and have to fly in harsh environments (e.g., low temperatures, low pressures and high UV radiation) for long periods (0.5–3 years). Therefore, the development of a durable stratospheric airship is quite challenging.

* To whom correspondence should be addressed. E-mail: inlee@kaist.ac.kr

Edited by the KSCM

DOI:10.1163/156855108X385285

Due to size and light structure requirements, a non-rigid structure type is preferred for an airship. In this case, the envelope is one of the major structural parts. The envelope contains the lifting helium gas and maintains the aerodynamic configuration of the airship. In addition, the envelope protects the airship from UV radiation, while it undergoes external forces, such as buoyancy, aerodynamic and inertia forces. The maximum size of a stratospheric airship envelope is expected to be 200 m in length and 50 m in diameter. It will be operated in a temperature range of −75 to 65°C. Therefore, the envelope material should not have significant material degradation or property changes, and it must sustain skin stress by superheating and by aerodynamic and inertial forces during operation. However, the envelope of a stratospheric airship is a specific application of a membrane that usually implies that it has a thin and low-modulus. Therefore, surface distortion of the structure may be easily induced by the boundary conditions, thickness variations, wrinkling, thermal distortions, membrane inflation level, and surface roughness in the membrane material itself. One of the most harmful situations for the membrane structure is the growth of wrinkling, as this phenomenon can rapidly induce the total collapse of the structure. For this reason, much research has been performed regarding the wrinkling phenomena [3–5].

In this research, the thermoelastic behaviors of an inflatable structure made of a fabric membrane to be applied in a stratospheric airship envelope are experimentally and numerically investigated. Mechanical tensile properties of the membrane material at room, high, and low temperature are measured using an Instron® universal testing machine and an Instron® thermal chamber. To characterize the nonlinear behaviors of the inflated membrane structure due to wrinkling, the bending behaviors of the inflated cylindrical boom made of the fabric membrane are experimentally and numerically investigated at various pressure levels. The inflated cylindrical boom is numerically modeled with the Stein–Hedgepeth membrane theory to describe the wrinkling behavior. The wrinkled area and deformed shapes are investigated by using the finite element program, ABAQUS. Moreover, the envelope of a stratospheric airship is numerically modeled based on the thermoelastic properties of the fabric membrane from experimental data and the wrinkled deformation induced by thermal load is analyzed.

2. Thermoelastic Properties of a Fabric Membrane

The schematic microstructure of the developed fabric membrane is illustrated in Fig. 1. The membrane was designed to consist of three layers: a load carrier, a helium barrier and a thermal bonding layer. The load carrier is composed of Vectran fiber plain weave fabric. Vectran is a high-performance thermoplastic multifilament yarn spun from Vectran liquid crystal polymer. Tedlar PVF film was selected for the helium barrier and the UV radiation protection. It was laminated to the load carrier fabric by using a polyurethane adhesive matrix. A thermoplastic polyurethane film (TPU, Dongsung chemical, Korea) was laminated at the inner

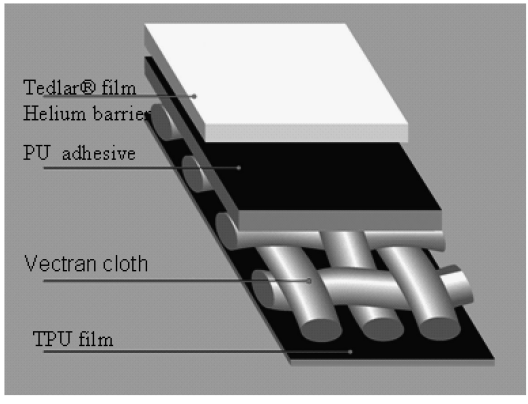

Figure 1. Microscopic structure of the fabric membrane for stratospheric airship.

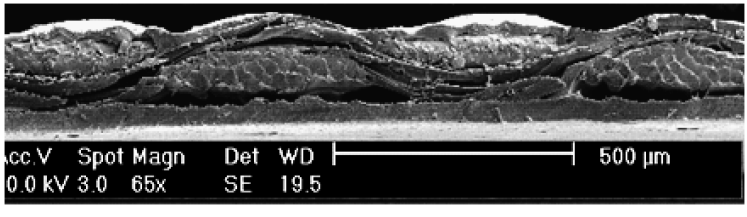

Figure 2. SEM image of the cross-section.

side for thermal bonding. The internal TPU layer plays an important role in blocking helium leakage if the external Tedlar layer is damaged. The scanning electron microscope (SEM) image of the membrane is shown in Fig. 2.

Figure 3 shows the experimental setup for the tensile test at various temperatures. Mechanical properties were measured by tensile tests in the temperature range of −75 to 65°C. First, the tensile test was done at room temperature (25°C), and the stiffness values were measured. Next, the experiment was performed at three low temperatures (−75°C, −50°C and −25°C) and at two high temperatures (50°C and 65°C). The specimens were fabricated by cutting the laminate into 25 mm × 150 mm sections. To prevent slipping during loading, #180 sand paper tabs were attached to each specimen grip. The sand papers were cured in an autoclave at 120°C under 3 atm for 2 h. For each temperature case, 5 specimens were tested. The tests were performed using an Instron® universal testing machine 4206 and an Instron® 3119–407 thermal chamber. Liquid nitrogen was used to achieve the low chamber temperature. The targeted chamber temperature was created with a ±2°C accuracy. The chamber was pressurized to 1.5 atm to stabilize the temperature. The specimens were pulled at the speed of 5 mm/min. The fabric membrane had an undulation on its surface due to the fiber architecture, which makes the use of a strain-gauge impractical for strain measurements. Therefore, the strains were measured with a 25 mm grip extensometer in this research.

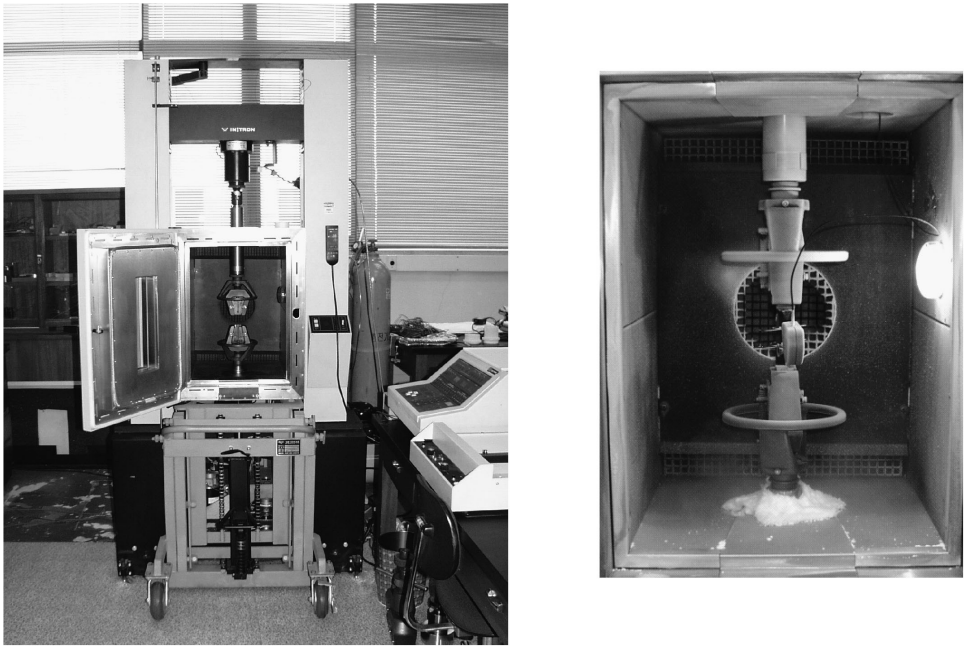

Figure 3. Experimental setup for tensile test at various temperatures.

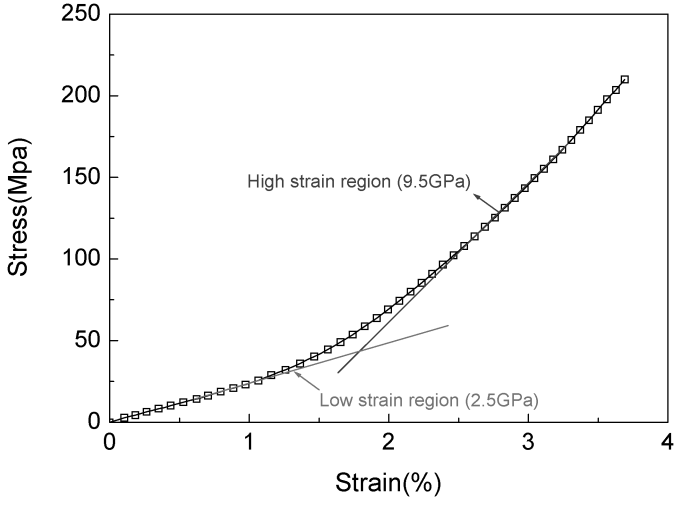

Figure 4. Stress–strain curve at room temperature.

The stress–strain curve for the tensile test at room temperature is shown in Fig. 4. The nominal stress–strain value is plotted, and the tensile modulus is calculated from the slope of the curve. As can be seen, the stress–strain curve of the material exhibits nonlinearity in the higher strain range. In the small strain region, the initially smaller stiffness increases rapidly as the tensile strain increases. However,

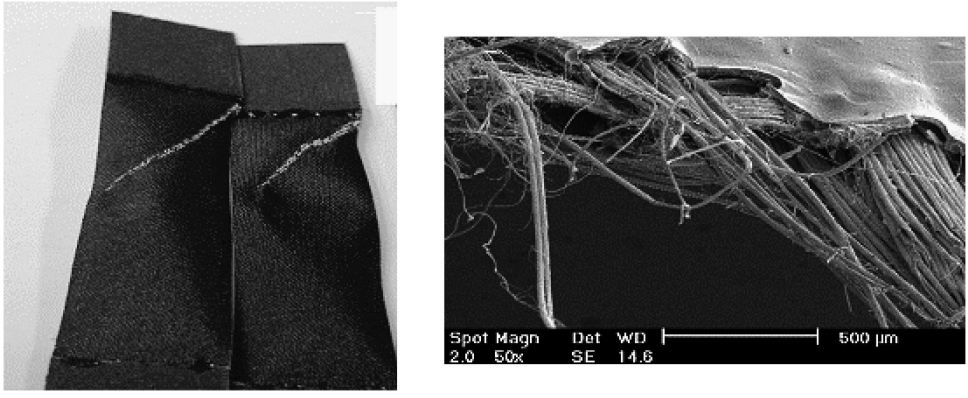

Figure 5. Failed specimens and SEM image of failed cross-section.

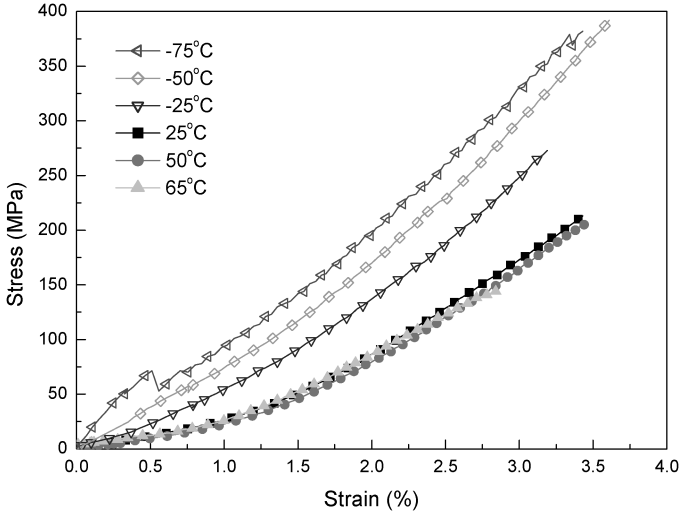

Figure 6. Stress–strain curves at various temperatures.

in the higher strain range, the rate of increase becomes smaller and the modulus reaches a steady-state value. In the low strain region, the value of the elastic modulus is about 2.5 GPa. Moreover, the steady-state modulus of about 9.5 GPa was determined in the strain range higher than 2.5%.

Figure 5 shows the failed specimens and the SEM cross-section image of a failed specimen. The figure shows that the failure started from the sand paper tabbed grip. The tensile failure stress was measured to be approximately 200 MPa which corresponded to 3.5% elongation.

Stress–strain curves measured at various temperatures are illustrated in Fig. 6, and the stiffness modulus calculated from the slopes of the curves is demonstrated in Fig. 7. The stiffness curves were obtained for decreasing temperatures, resulting in higher moduli. The steady-state stiffness modulus obtained for the lowest

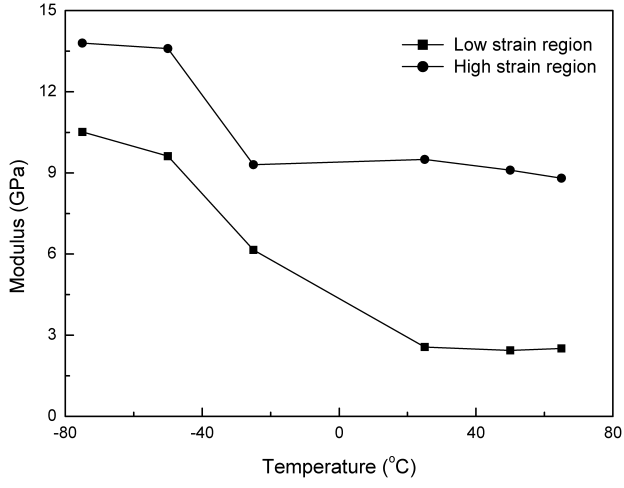

Figure 7. Variation of the tensile modulus at various temperatures.

temperature (−75°C) is 45% larger than that obtained at room temperature (25°C). This was expected, since the stiffness modulus of Vectran fiber is known to increase by 40% at low temperatures.

3. Nonlinear Behaviors of Inflated Membrane Boom

To characterize the nonlinear behaviors of the inflated membrane structure due to wrinkling, an inflated cylindrical boom was numerically modeled, and the results were compared with experimental data.

3.1. Membrane Model With Wrinkling

To consider the wrinkling of a membrane, the wrinkling model of Stein–Hedgepeth [6] was applied. This wrinkle theory applies to membranes that are elastic, isotropic, have no bending stiffness and cannot carry compressive stress. A numerical algorithm that retains the nonlinear wrinkle model may be expressed as:

$$\boldsymbol{\sigma} = \mathbf{D}\boldsymbol{\varepsilon}, \tag{1}$$

where $\boldsymbol{\sigma} = \{\sigma_{xx},\ \sigma_{yy},\ \tau_{xy}\}^{\mathrm{T}}$, $\boldsymbol{\varepsilon} = \{\varepsilon_{xx},\ \varepsilon_{yy},\ \gamma_{xy}\}^{\mathrm{T}}$, and $\mathbf{D}$ is a local 'equivalent elasticity' matrix that relates stresses $\boldsymbol{\sigma}$ and elastic strain $\boldsymbol{\varepsilon}$ within a membrane element. A useful algorithm for choosing the $\mathbf{D}$ matrix, the stress–strain criteria, is used [7]:

Stress–strain criteria

$$\sigma_2 > 0\text{: taut}, \tag{2a}$$

$$\varepsilon_1 \leqslant 0\text{: slack}, \tag{2b}$$

$$\varepsilon_1 > 0 \text{ and } \sigma_2 \leqslant 0\text{: wrinkled}, \tag{2c}$$

where σ_2 and ε_1 are the minor principal stress, and major principal strain, respectively. If both principal stresses are tensile, then the membrane is taut. If both principal stresses are zero, then the membrane is slack. However, if one principal stress (minor) is zero and the other (major) is tensile, then the membrane wrinkles. The effective elasticity matrix at each membrane state can be expressed as follows:

$$\mathbf{D}_{\text{Taut}} = \frac{E}{1-\nu^2}\begin{bmatrix} 1 & \nu & 0 \\ \nu & 1 & 0 \\ 0 & 0 & \dfrac{1-\nu}{2} \end{bmatrix}, \tag{3a}$$

$$\mathbf{D}_{\text{Slack}} = \begin{bmatrix} 0 & 0 & 0 \\ 0 & 0 & 0 \\ 0 & 0 & 0 \end{bmatrix}, \tag{3b}$$

$$\mathbf{D}_{\text{Wrinkled}} = \frac{E}{4}\begin{bmatrix} 2(1+P) & 0 & Q \\ 0 & 2(1-P) & Q \\ Q & Q & 1 \end{bmatrix}, \tag{3c}$$

where $P = \cos(2\alpha)$, $Q = \sin(2\alpha)$ and α is the principal angle. The taut matrix (equation (3a)) follows the linear elastic isotropic material constitutive formulation. The slack matrix (equation (3b)) formulation is based upon the assumption that no stress is formed in a slack region. The wrinkled matrix (equation (3c)) is formulated from the constitutive relations by using the variable Poisson's ratio [6]. The numerical analysis involves nonlinear stress–strain behavior, so that an iterative solution is required. The resulting model is analyzed with the same loads, and the process is repeated until no compressive stresses remain in the membrane. To simulate a wrinkling phenomenon, the numerical algorithm of wrinkling based on the Stein–Hedgepeth membrane model is developed and implemented *via* a user subroutine (UMAT) supported by the ABAQUS finite element program (Fig. 8). In this model, membrane states, such as taut, wrinkled, and slack are calculated at each load step by using stress–strain criteria (equations (2a)–(2c)) and the Stein–Hedgepeth wrinkling model (equations (3a)–(3c)).

3.2. Inflated Cylindrical Boom in Bending

The bending behavior of inflated cylindrical boom structures was experimentally and numerically investigated. The experimental model was established from the fabric membrane. In the numerical analysis, the wrinkling model of Stein–Hedgepeth [6] with membrane elements was applied.

The bending test was carried out on inflated cylindrical booms with various internal pressures. The test frame was designed to measure the deflection of the end tip when it was loaded in a lateral direction (Fig. 9). A load was applied *via* weighting at the tip of the boom, which was covered with an acryl hoop. Tip deflection was measured by a laser sensor and recorded using a data acquisition system. Ni-

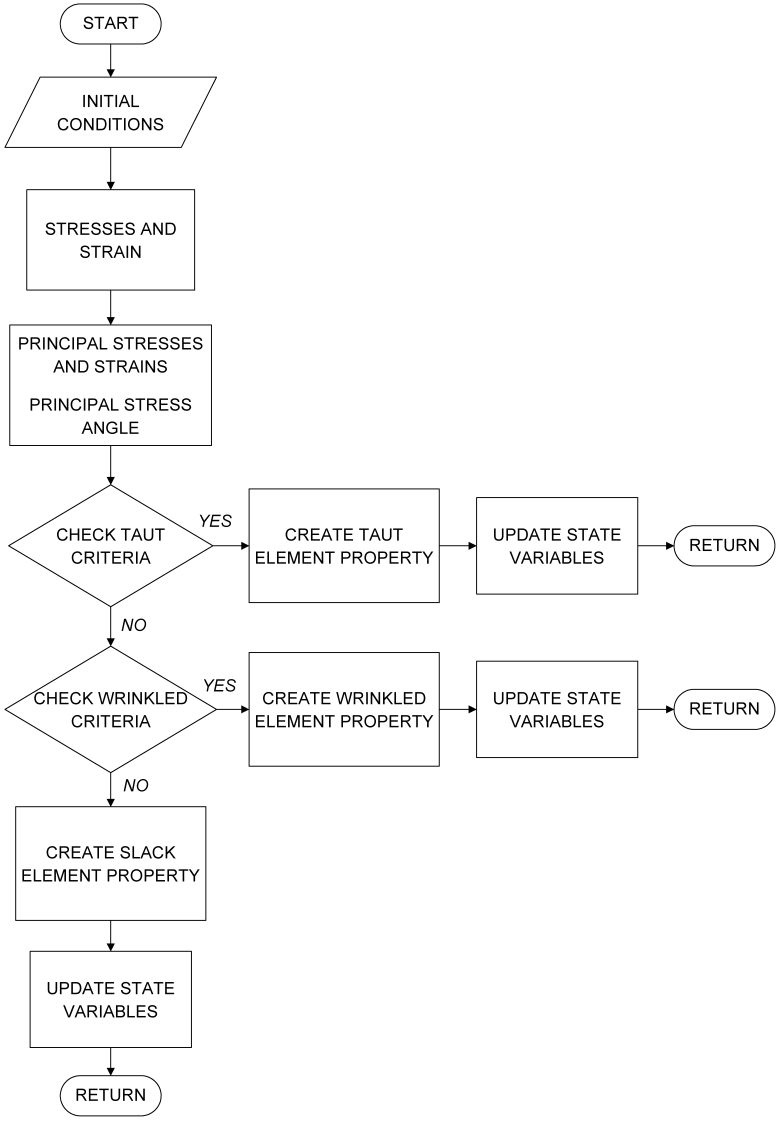

Figure 8. Flow chart of wrinkling algorithm.

trogen gas was used as the inflation gas, and the internal pressure was measured by a pressure sensor.

Figure 10 shows a numerical model of the inflated cylindrical boom. A rigid body constraint was applied to the upper edge. When the boom structure was pressurized, the membrane was tensioned longitudinally as well as laterally. Considering the pressure load to the upper end cap surface, the stretching force (F_s) was applied. The thickness, Young's modulus, and Poisson's ratio of the fabric laminated membrane were $t = 200$ μm, $E = 2.5$ GPa and $\nu = 0.34$, respectively. Even if an internal

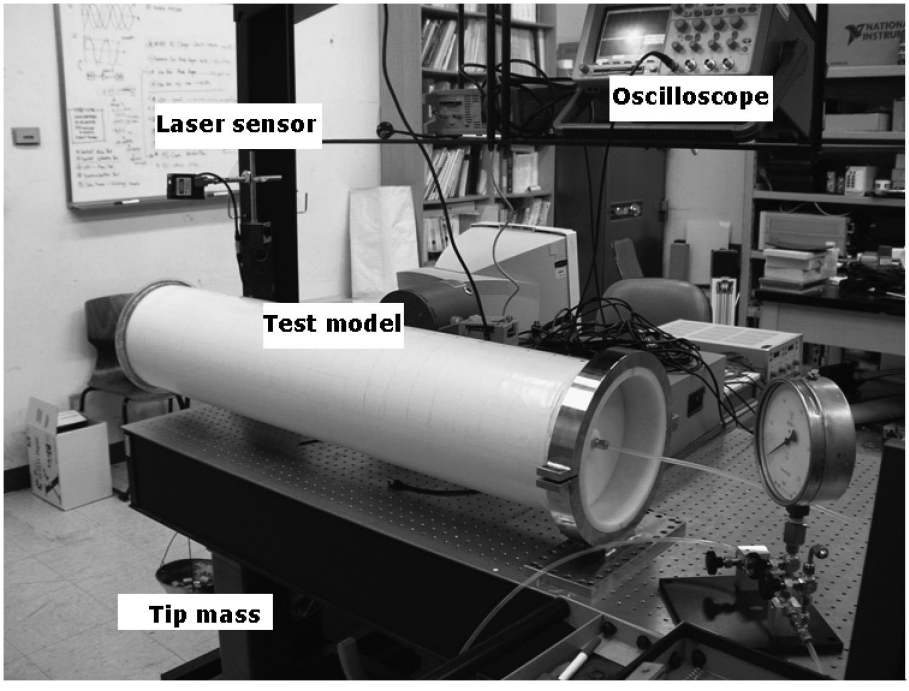

Figure 9. Experimental setup for the inflatable boom structure in bending.

pressure was applied in the inflated boom structure, the longitudinal elongation of the membrane was within 2.5%. Therefore, the value of an elastic modulus in the low strain region was used. In the finite element analysis, the Stein–Hedgepeth membrane model using 660 membrane elements (M3D4) was applied. The membrane states of taut, slack, and wrinkled were calculated at each load step. To reduce the computational time, a mesh having 33 elements in the length direction and 20 around the circumference was applied.

The load and deflection curves with internal pressure were investigated for the slenderness ratio $2L/D = 9.6$ (length, $L = 1.2$ m and diameter, $D = 0.25$ m). As can be seen from Fig. 11, there were very good correlations between the numerical and experimental results, even if there was some deviation in the linear deflection region because the mass effect of the end cap cannot be considered in the numerical model of the inflated boom. By increasing internal pressure, the critical load required to initiate collapse is also increased. Expansion of the wrinkling area and the deformation of the inflated membrane boom were observed. As can be seen from Fig. 12, the wrinkled area develops at the bottom region along the circumferential direction, according to the deflection increase. The membrane elements at the bottom region totally collapse due to wrinkling extension. Therefore, the wrinkled elements cannot sustain the applied load any longer and simply play the role of a hinge. The experimentally observed wrinkled region can be seen in Fig. 13.

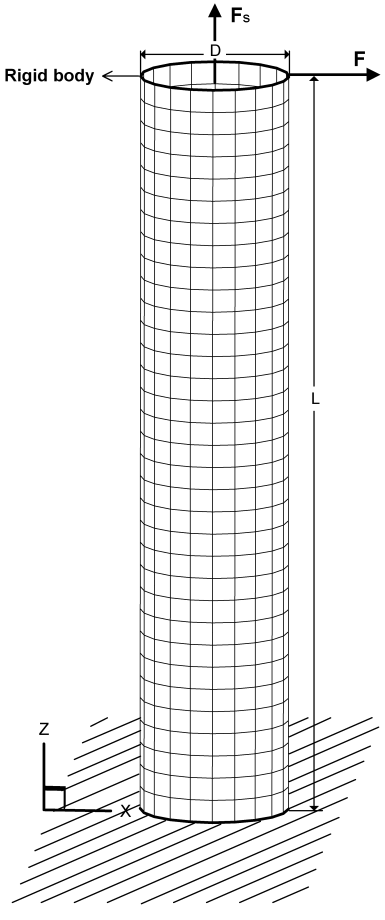

Figure 10. Inflated cylindrical boom model.

4. Numerical Analysis of the Stratospheric Airship Envelope

The envelope of a stratospheric airship is numerically modeled, and its thermoelastic behaviors are investigated. A hull of a large airship envelope is modeled as a membrane. Figure 14 shows the numerical model of a stratospheric airship envelope (a length $L = 50$ m and a diameter $D = 12.5$ m) using 2.208 membrane elements (M3D4) supported by ABAQUS. For the numerical analysis, the variation of modulus in the low strain region is represented by using a linear function, as shown in Fig. 15. The value of the thermal expansion coefficient, $\alpha = -0.26$ μ/°C, was determined by using the rule of mixture based on the properties of Tedlar film, Vectran fiber and TPU film. The stiffness is strongly dependent on the temperature showing a large amount of change as the temperature is varied. Therefore, it is important to analyze the thermoelastic behavior of the stratospheric airship envelope, which experiences a wide range of temperatures moving from sea level to the stratosphere. It is assumed that the environmental temperature of an airship is

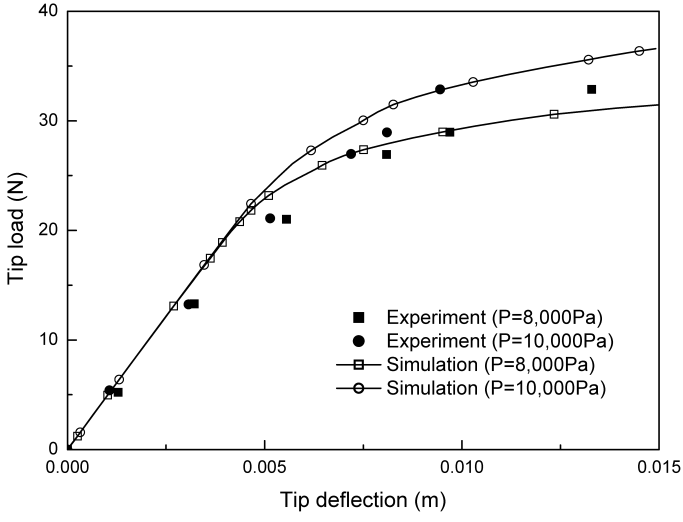

Figure 11. Load–deflection curves with various internal pressures.

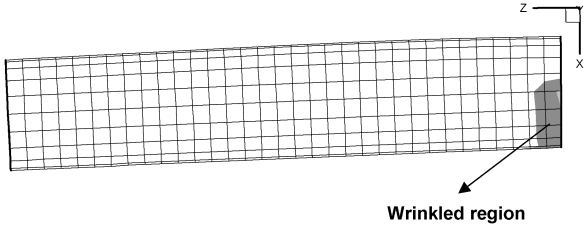

Figure 12. Wrinkled deformation at tip deflection of 0.012 m (internal pressure = 10 000 Pa).

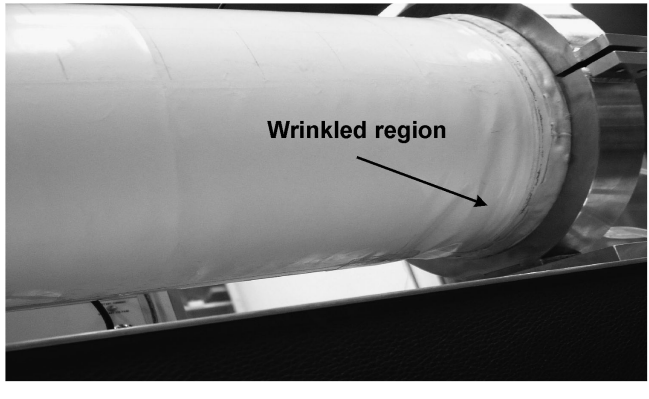

Figure 13. Experimentally wrinkled region (internal pressure = 10 000 Pa).

equal to −60°C, and the temperature of the top surface should be increased to 70°C due to solar heat radiation. We investigated the wrinkled deformations induced by a thermal load when an internal pressure of 5 Pa is applied to the envelope of an

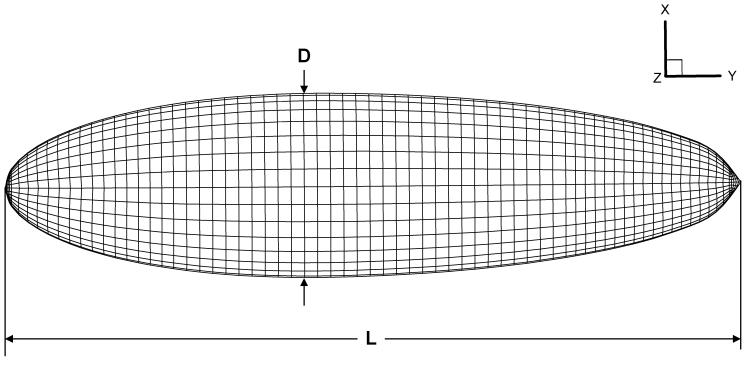

Figure 14. Numerical model of stratospheric airship envelop.

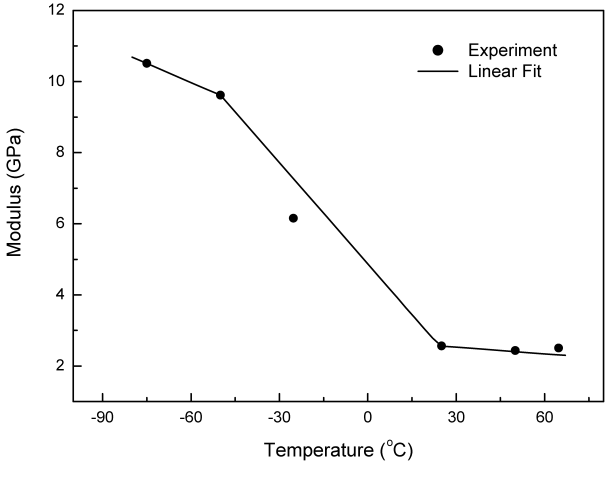

Figure 15. Linear functional model of the modulus in the low strain region.

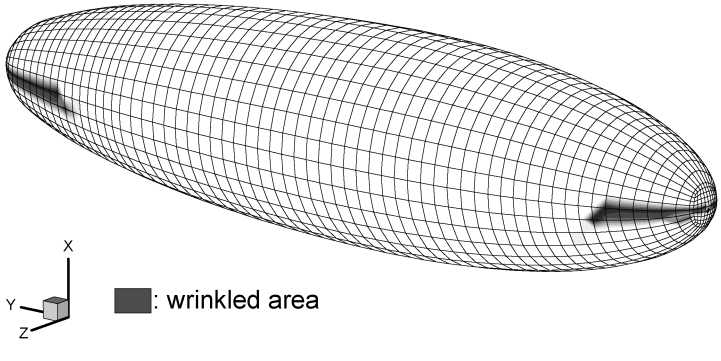

Figure 16. Wrinkled area of airship.

airship. Figure 16 illustrates the wrinkled region. The expansion of the wrinkling area can induce structural instability, while the shape deformation induced by a

thermal load can change the aerodynamic characteristics of an airship. Therefore, a deformation analysis considering the wrinkling effect is one of the most important procedures to be performed before the design and manufacturing of a stratospheric airship envelope.

5. Conclusion

In this study, thermoelastic behaviors of an inflatable structure made of a fabric membrane designed for use in a stratospheric airship envelope were experimentally and numerically investigated. Mechanical tensile properties of the membrane material at room, high, and low temperatures were measured using an Instron® universal testing machine and an Instron® thermal chamber. The inflated membrane structures, a cylindrical boom and a stratospheric airship envelope, were numerically modeled based on the thermoelastic properties of a fabric membrane obtained from experimental data. Moreover, the nonlinear characteristics of the membrane structures due to the wrinkling were investigated by using the Stein–Hedgepeth membrane theory.

The tensile test results for the fabric membrane showed significant nonlinearity in the strain–stress behavior. It was also found that the modulus was strongly dependent on the environmental temperature, showing a large amount of change as the temperature was varied. Moreover, due to wrinkling, the inflated cylindrical boom made of the fabric membrane showed high nonlinearity in the bending test. A wrinkling analysis is very important in the design procedure of inflatable structures, because the growth of wrinkling can rapidly induce the total collapse of a structure. Especially, in a stratospheric airship envelope, the expansion of a wrinkling area can induce structural instability, while the shape deformation induced by a thermal load can change the aerodynamic characteristics of the airship. Therefore, a deformation analysis considering the wrinkling effect is one of the most important procedures to be performed before the design and manufacturing of a stratospheric airship envelop.

Acknowledgements

This work was supported by the second stage of the Brain Korea 21 Project in 2007. The authors also acknowledge the support by the Korea Aerospace Research Institute.

References

1. A. Nayler, Airship activity and development world-wide-2003, *AIAA's 3rd Aviation Technology, Integration and Operations (ATIO) Technical Forum*, Denver, CO, USA (2003).
2. Y.-G. Lee, D.-M. Kim and C.-H. Yeom, Development of Korea high altitude platform systems, *Intl J. Wireless Info. Networks* **13**, 31–42 (2006).

3. C. M. Jenkins, Gossamer spacecraft: membrane and inflatable structures technology for space applications, *Progress in Astronautics and Aeronautics*, Vol. 191, American Institute of Aeronautics and Astronautics, USA (2000).
4. J. R. Blandino, J. D. Johnston, J. J. Miles and U. K. Dharamsi, The effect of asymmetric mechanical and thermal loading on membrane wrinkling, *Proc. 43rd AIAA/ASME/ASCE/AHS/ASC Structures, Structural Dynamics and Materials Conference*, Denver, CO, USA (2002).
5. E.-J. Yoo, J.-H. Roh and J.-H. Han, Wrinkling control of inflatable booms using shape memory alloy wires, *Smart Mater. Struct.* **16**, 340–348 (2007).
6. M. Stein and J. M. Hedgepeth, Analysis of partly wrinkled membranes, Technical Note, *NASA TN D-813* (1961).
7. S. Kang and S. Im, Finite element analysis of dynamic responses of wrinkling membranes, *Comput. Methods Appl. Mech. Engng* **173**, 227–240 (1999).